

Gate-controlled spin-orbit interaction in a parabolic GaAs/AlGaAs quantum well

M. Studer*,^{1,2} G. Salis†,¹ K. Ensslin,² D. C. Driscoll,³ and A. C. Gossard³

¹*IBM Research, Zurich Research Laboratory, Säumerstrasse 4, 8803 Rüschlikon, Switzerland*

²*Solid State Physics Laboratory, ETH Zurich, 8093 Zurich, Switzerland*

³*Materials Department, University of California, Santa Barbara, California 93106, USA*

We study the tunability of the spin-orbit interaction in a two-dimensional electron gas with a front and a back gate electrode by monitoring the spin precession frequency of drifting electrons using time-resolved Kerr rotation. The Rashba spin splitting can be tuned by the gate biases, while we find a small Dresselhaus splitting that depends only weakly on the gating. We determine absolute values and signs of the two components and show that for zero Rashba spin splitting the anisotropy of the spin dephasing rate vanishes.

Spin-orbit (SO) interaction is one of the key ingredients for future spintronic devices. In a two-dimensional electron gas (2DEG), SO interaction manifests itself as a spin splitting, and two different asymmetries can be responsible for it: The inversion asymmetry of a zincblende crystal leads to the so-called Dresselhaus spin splitting [1], and an electric field, E_{QW} , along the growth direction enables Rashba-type spin splitting [2]. E_{QW} is either generated by an asymmetrically grown layer structure (e.g., doping profile), or can be controlled externally by appropriate gating. The latter allows for a very efficient and scalable approach to control spins [3, 4].

The possibility of tuning the SO interaction in a 2DEG with a front gate (FG) electrode was first exploited by Nitta et al. [5], who studied Shubnikov–de Haas (SdH) oscillations. Similar experiments were done in a 2D hole system with a FG and a back gate (BG) electrode [6]. These experiments could not differentiate between the Dresselhaus and Rashba components. By tuning the sheet density of a 2DEG and a careful analysis of weak antilocalization peaks, Rashba and Dresselhaus SO interaction were separated in a transport experiment [7]. It has been proposed that such information could also be obtained from measurements of conductance anisotropy in quantum wires [8]. Using photocurrents, it is possible to characterize the sources of SO interaction, but not to make a quantitative statement about the SO strength [9, 10]. In a 2DEG, the spin lifetime, which can be measured optically, is limited mainly by the Dyakonov–Perel (DP) dephasing mechanism [11] and therefore by the strength of the SO interaction. An optical study of the spin lifetime as a function of gate voltages therefore indirectly provides information on the tunability of the SO interaction [12, 13].

A more direct method to obtain quantitative access to both the Rashba and the Dresselhaus SO interaction strength is to measure the drift-induced effective SO magnetic field (in the following referred to as SO field) [14].

Here, we employ this method to study the tunability of the SO interaction by means of an external electric field, E_{ext} , perpendicular to the plane of a 2DEG confined in a parabolic potential. By using FG and BG electrodes, independent control of both E_{ext} and the carrier sheet density [15] is obtained. Although the electrons are confined in a parabolic well that does not change its shape with bias, we find a Rashba SO field that depends linearly on E_{ext} . The Dresselhaus SO field is only weakly affected by the gate bias. Together with a measurement of the mobility of the 2DEG, we obtain quantitative values for the Rashba coupling and its sign. Our optical measurements allow the simultaneous determination of the different contributions to SO interaction and the spin lifetime. In agreement with the DP dephasing mechanism [13, 16], the in-plane anisotropy of the spin lifetime disappears when $\alpha = 0$, validating previous experiments that extracted ratios of SO splittings from measurements of spin-dephasing. [13]

The structure measured is a molecular-beam epitaxy-grown $\text{Al}_x\text{Ga}_{1-x}\text{As}$ quantum well (QW) with parabolic confinement [15, 17]. The QW is 100 nm thick, and the Al concentration varies from $x = 0$ in the center of the well (located $d_{FG} = 105$ nm below the surface) to $x = 0.4$ at the edges. The QW is modulation doped with Si on both sides. A 490 nm thick layer of low-temperature-grown GaAs isolates the QW from the BG, which consists of a highly n -doped GaAs layer and is located $d_{BG} = 1100$ nm below the QW, see Fig. 1(b). Using photolithography and wet etching, a cross-shaped mesa structure [see Fig. 1(a)] with standard AuGe Ohmic contacts to the 2DEG and the BG is defined. A semi-transparent FG consisting of a 2 nm Ti adhesion layer and 6 nm of Au covers the cross. We characterize the electronic properties of the sample at 30 K in a magnetic field perpendicular to the sample plane, using the lower arm of the cross as a Hall bar. From measurements in the dark and under illumination, we find a persistent photoconduction that increases the carrier sheet density in the QW by a factor of about two and lowers the effectiveness of the gates under illuminated conditions. Both effects are attributed mainly to the ionization of DX centers in

*mattstud@phys.ethz.ch

†GSA@zurich.ibm.com

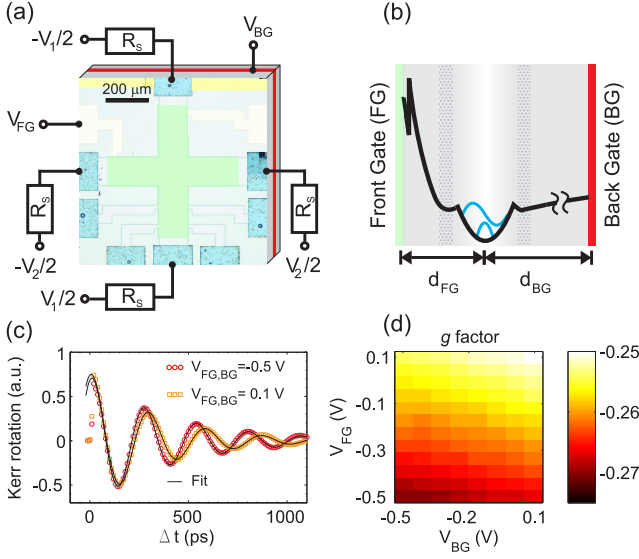


FIG. 1: (color online) (a) False-color image of the sample as seen in an optical microscope: Cross-shaped mesa structure covered by a FG (green) and Ohmic contacts on each end (blue). The BG is indicated in red. (b) Schematic conductance-band profile of the grown layer structure including gate electrodes and wave functions of the two occupied subbands. (c) TRKR for $V_{FG} = V_{BG} = -0.5$ V and 0.1 V, respectively. (d) g factor of the electrons confined in the QW as a function of the gate voltages.

the doping layers. After illumination, the sheet density is tunable between $7.1 \times 10^{11} \text{ cm}^{-2}$ and $7.5 \times 10^{11} \text{ cm}^{-2}$ by applying bias voltages V_{FG} between the FG and the 2DEG as well as V_{BG} between the BG and the 2DEG. At 2.4 K, SdH oscillations in $1/B$ exhibit a beating that corresponds to two frequencies, indicating that two subbands are occupied [15]. The sum of its sheet densities, extracted from the SdH oscillations, equals the Hall density. From this, we conclude that a possible parallel conductivity layer has a much lower mobility than the 2DEG. In the experiments presented in the following, the 2DEG is in the illuminated state.

We use time-resolved Kerr rotation (TRKR) to probe the spin dynamics of the carriers confined in the QW [14]. The pump pulses (average power $700 \mu\text{W}$; repetition rate 80 MHz) are focused on a $30\text{-}\mu\text{m}$ -wide spot in the center of the cross. The probe beam ($70 \mu\text{W}$) is focused onto the same spot. The TRKR signal is well described by an exponentially decaying cosine $A \exp(-\Delta t/T_2^*) \cos(g\mu_B B_{tot} \Delta t/\hbar)$, where A is the amplitude of the Kerr signal, T_2^* the ensemble spin lifetime, g the electron-spin g factor, μ_B the Bohr magneton, and B_{tot} is the total magnetic field that is composed of an external magnetic field, B_{ext} , and a SO field [14]. The measurement of the SO interaction relies on the fact that the SO field and thus B_{tot} depend on the direction and magnitude of the electron drift, induced by applied voltages $V_1 = V_0 \cos(\varphi)$ and $V_2 = V_0 \sin(\varphi)$ symmetrically to the four

arms of the cross via serial resistors $R_S = 4.7 \text{ k}\Omega$, see Fig. 1(a). This creates a well-controlled in-plane electric field $\mathbf{E}_D(\varphi, V_0)$ in the center of the cross [18]. The application of \mathbf{E}_D breaks the symmetry in k space and shifts the electron population in the s -th subband by $\delta \mathbf{k}_s = -m^* \mu_s \mathbf{E}_D/\hbar$, where μ_s is the mobility of the subband and m^* the electron effective mass. Because of this, the average spin of the electrons in this subband is exposed to an effective magnetic field that can be divided into a Dresselhaus term $\mathbf{B}_{D,s}$ and a Rashba term $\mathbf{B}_{R,s}$:

$$\mathbf{B}_{D,s} = \frac{2\beta_s}{g_s \mu_B} \begin{pmatrix} \delta k_{y,s} \\ \delta k_{x,s} \end{pmatrix} \quad \mathbf{B}_{R,s} = \frac{2\alpha_s}{g_s \mu_B} \begin{pmatrix} \delta k_{y,s} \\ -\delta k_{x,s} \end{pmatrix}. \quad (1)$$

We use a coordinate system with $x||[1\bar{1}0]$, $y||[110]$ and $z||[001]$, and restrict our discussion to two subbands. For two occupied subbands there is an additional contribution to the SO interaction [19], that, however, depends only weakly on E_{ext} and would appear in our measurements as a constant contribution to the Rashba SO field. Typical inter-subband scattering times are on the order of ps [20], which is two orders of magnitude faster than the spin precession period in our experiment. This implies that one precessing electron spin is on average equally present in both subbands during its lifetime and that therefore the TRKR signal represents an average of the two occupied subbands. Only one Larmor frequency is observable, even if the g factors of the two subbands are different. As pointed out in Ref. 21, the fast intersubband scattering is also a source of spin decoherence. Assuming that both subbands contribute equally to the TRFR signal, we measure a SO field that is proportional to the average SO field of the two subbands: $\mathbf{B}_D = (\mathbf{B}_{D,1} + \mathbf{B}_{D,2})/2$ and $\mathbf{B}_R = (\mathbf{B}_{R,1} + \mathbf{B}_{R,2})/2$. We apply \mathbf{B}_{ext} in the plane of the 2DEG at an angle θ with respect to the x axis. If $B_{ext} \gg B_D$ and B_R , B_{tot} can be approximated by [14]

$$B_{tot}(\theta, \phi) \approx B_{ext} + (B_D + B_R) \cos \theta \sin \varphi + (B_D - B_R) \sin \theta \cos \varphi. \quad (2)$$

Because of the different symmetries, the drift-induced modification of B_{tot} is proportional to $B_D + B_R$ for $\theta = 0^\circ$, and to $B_D - B_R$ for $\theta = 90^\circ$.

All the experiments are carried out at 30 K and with $B_{ext} = 0.987 \text{ T}$. Figure 1(c) shows the TRKR signal as a function of the pump-probe delay for two gate configurations ($V_{FG} = V_{BG} = -0.5$ and 0.1 V). The signals are well fit by an exponentially decaying cosine, and as B_{ext} is known, the g factor can be obtained. Figure 1(d) shows the g factor as a function of the gate voltages. We assume that it is negative [17]. The g factor becomes less negative both for increasing V_{FG} and for increasing V_{BG} , indicating that a larger carrier sheet density and therefore a higher energy of the electrons are the main cause [22]. A lateral displacement of the subband wave

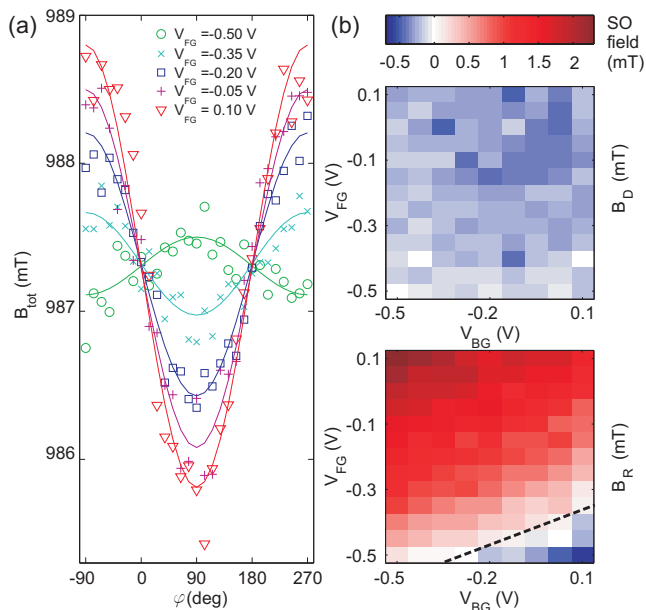


FIG. 2: (color online) (a) B_{tot} for $V_{BG} = -0.375$ V and different V_{FG} biases. The magnetic field is applied in the $\theta = 180^\circ$ direction. The amplitude of the oscillation in φ , including its sign, is tunable with the FG. (b) Experimentally obtained SO fields as a function of V_{FG} and V_{BG} . Tuning of the symmetry of the QW allows B_R to be tuned over a large range, including a sign change (dashed line), whereas B_D shows only small variations.

function should also change g and manifests itself in a dependence where V_{FG} and V_{BG} modify the g factor into opposite directions [17]. The latter effect plays a minor role in our doped sample, in contrast to the undoped samples studied in Ref. 17.

Figure 2(a) displays the measured B_{tot} as a function of the angle φ of the direction of $\delta\mathbf{k}$ for $V_0 = 1.8$ V, where $E_D \approx 87$ V/m in the center of the cross. Gating-induced variations of E_D and the mobility result in a variation in δk below 5%. The geometry of our sample keeps the density in the center of the cross constant during a φ rotation, preventing a g factor modulation. To test this, we apply B_{ext} in the opposite direction and find the same oscillation in φ with a sign-reversed amplitude, consistent with Eq. (2) (data not shown). The solid lines are fits using Eq. (2). As $\theta = 180^\circ$, B_{tot} oscillates in φ with an amplitude given by $B_D + B_R$. As seen in Fig. 2(a), this amplitude strongly depends on the V_{FG} applied, suggesting a large variation in the SO interaction. The SO field does not depend on the magnitude of B_{ext} , and no pump-power dependence of the measured SO fields is observed [18]. The same measurements were done in one cool-down for a matrix of FG and BG voltages for two samples glued onto the same chip carrier but with different orientations of the crystallographic axes such that $\theta = 180^\circ$ and $\theta = 90^\circ$, respectively. From these measurements, B_D and B_R can be obtained separately [See

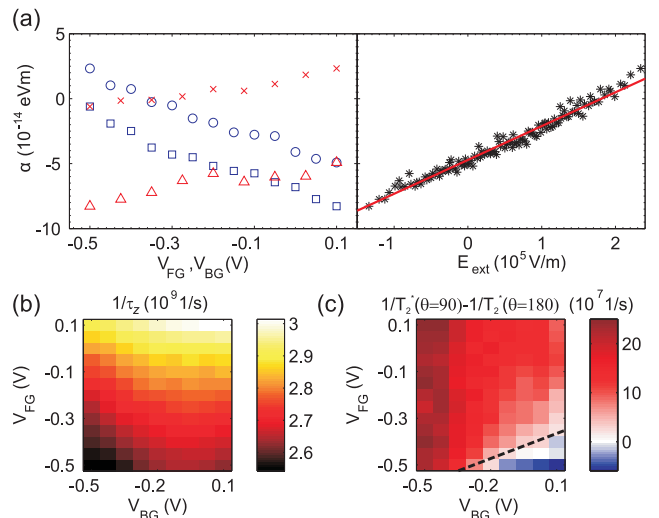


FIG. 3: (color online) (a) Left panel: α as a function of the FG (BG) voltage with fixed BG (FG) voltage (Δ : $V_{FG} = 0.1$ V; \times $V_{FG} = -0.5$ V; \circ : $V_{BG} = 0.1$ V; \square : $V_{BG} = -0.5$ V). Right Panel: α as a function of E_{ext} . The red line represents a least-squares fit as described in the text. (b) Averaged spin-dephasing rate for $\theta = 90^\circ$ and $\theta = 180^\circ$ (c) In-plane spin-dephasing asymmetry. The dashed line marks the same gate voltage regime as in Fig. 2(b).

Fig. 2(b)]. We observe a large variation in B_R , including a sign change (dashed line). V_{BG} and V_{FG} have the opposite effect on B_R , suggesting that a tuning of the symmetry is responsible for the variation. Compared to B_R , B_D is rather constant. In the following we will first discuss B_R and then come back to B_D .

An electric field E_{ext} applied perpendicularly to the plane of the QW shifts the potential minimum along the z direction, but does not change the shape of the parabolic confinement [15]. Nevertheless it is expected that the Rashba SO coefficient α changes linearly [23], $\alpha = E_{QW}r_{QW}$. This can be explained by the notion that the electric field in the valence band determines the Rashba splitting in the conduction band [23]. Here, r_{QW} is a constant that depends on the material of the QW and $E_{QW} = E_{ext} + E_{AP}$ can either be generated by an asymmetrically grown potential (E_{AP}) or by gating the structure (E_{ext}). E_{ext} is related to V_{BG} and V_{FG} by

$$E_{ext} = \frac{V_{BG}}{f_{BG}d_{BG}} - \frac{V_{FG}}{f_{FG}d_{FG}}, \quad (3)$$

where f_{BG} and f_{FG} are screening factors of the BG and the FG, respectively.

As δk_s is given by the measured mobility and E_D , $\alpha = (\alpha_1 + \alpha_2)/2$ can be obtained from B_R , assuming that the mobility is the same in both subbands. In the left panel of Fig. 3(a), we plot α as a function of $V_{FG(BG)}$, while $V_{BG(FG)}$ is kept fixed. We find parallel lines for two BG (FG) sweeps, suggesting a linear dependence of α on the gate voltages, as predicted by Eq. (3). E_{ext} can

be estimated by evaluating the density dependence of the 2DEG on V_{FG} and V_{BG} and comparing it with a plate capacitor model [6]. In the dark we find $f_{BG} = f_{FG} = 1$, i.e. no screening is observed. Under illumination, f_{FG} is between 15 and 20 and $f_{BG} \approx 5$. We plot all B_R data points as a function of E_{ext} by fixing $f_{BG} = 5$ and treating f_{FG} as a fitting parameter to fit all points to one line [see right panel of Fig. 3(a)]. This yields $f_{FG} = 21$, which is similar to the value obtained from the density dependence, indicating that α is mainly governed by E_{ext} and much less so by the density. The sign change of α is explained by a change of the symmetry of the QW. From the slope in Fig. 3(a), $r_{QW} = 25 \text{ e}\text{\AA}^2$ is extracted. This is on the same order of magnitude as $5 \text{ e}\text{\AA}^2$, the value cited for GaAs in Ref. 23. α is positive for E_{QW} pointing from the substrate to the surface.

In Fig. 3(b) we plot the average of two spin-dephasing rate measurements $1/T_2^*$ with $\theta = 90^\circ$ and $\theta = 180^\circ$, which is equivalent to the spin-dephasing rate in the z direction, $1/\tau_z$. A higher dephasing rate is observed for higher densities, as expected from the DP mechanism [16]. In Fig. 3(c), the difference of these two measurements is plotted. The in-plane anisotropy of the spin-dephasing results from the interplay between the two SO contributions [13, 18]. From theory, a vanishing anisotropy is expected for $\alpha = 0$ [16]. The dashed line in Fig. 3(c) indicates bias regions with no Rashba spin splitting, corresponding also to the region where the in-plane anisotropy of the spin decay disappears, confirming the theory and supporting our measurements of α .

We now come back to discuss the size of B_D , which can be understood by taking the full Dresselhaus term into consideration. Starting with the cubic Dresselhaus term [16], we include the confinement in the x - y plane by replacing k_z^2 by the expectation value $\langle k_{z,s}^2 \rangle$ of the s -th quantized subband wave function. Integrating the effective magnetic field over the shifted Fermi circle using $\delta k_s \ll k_{F,s}$ yields the Dresselhaus SO field including the higher-order terms

$$\mathbf{B}_{D,s} = \frac{2\gamma_s}{g_s\mu_B} (k_{F,s}^2/4 - \langle k_{z,s}^2 \rangle) \begin{pmatrix} \delta k_{y,s} \\ \delta k_{x,s} \end{pmatrix}, \quad (4)$$

where γ_s is a material-dependent parameter [24] and $k_{F,s} = \sqrt{2\pi n_s}$ is the Fermi wave vector of the s -th subband with the subband density n_s . Interestingly, two terms contribute to the SO field: one proportional to $\langle k_{z,s}^2 \rangle$ and one proportional to $k_{F,s}^2$. For sufficient confinement, $\langle k_{z,s}^2 \rangle \gg k_{F,s}^2$, Eq. 1 is recovered with $\beta_s = -\gamma_s \langle k_{z,s}^2 \rangle$.

To estimate B_D with Eq. 4 we use the SdH densities at 2.4 K, $n_1 = 4.2$ and $n_2 = 2.3 \times 10^{15} \text{ m}^{-2}$ and extrapolate them to the Hall density $7.3 \times 10^{15} \text{ m}^{-2}$ measured at 30 K. A numerical simulation of the wave functions in the QW yields $\langle k_{z,1}^2 \rangle = 2.2 \times 10^{15} \text{ m}^{-2}$ and $\langle k_{z,2}^2 \rangle = 7.5 \times 10^{15} \text{ m}^{-2}$. With a measured mobility of $8.2 \text{ m}^2/\text{Vs}$ at

30 K, assuming that both subbands have this mobility and $\gamma_s = 10^{-30} \text{ eVm}^3$, taken from literature [25], Eq. (4) predicts a value of $-0.4 \pm 0.5 \text{ mT}$ for B_D . This is in good agreement with the measured $B_D \approx -0.3 \text{ mT}$ at $V_{FG} = V_{BG} = 0 \text{ V}$. The contributions of the two subbands have opposite sign, leading to this small value. In Fig. 2(b) B_D tends to slightly more negative values with positive gating. This trend is explainable by the higher density and thus higher $k_{F,s}$ and the small confinement leading to a lower $\langle k_{z,s}^2 \rangle$ because of the screening of the parabola by the electrons.

To conclude, we have measured the SO field originating from the Dresselhaus and the Rashba SO interaction in a system where an electric field E_{ext} perpendicular to the QW plane as well as the carrier sheet density can be controlled with a FG and a BG. A small Dresselhaus SO field and a Rashba-induced SO field that linearly depends on E_{ext} are found. Taking into account the two occupied subbands, the small values of the Dresselhaus SO field can be understood qualitatively. We determine the sign of subband-averaged α and show full tunability of α through zero. This result is confirmed by a vanishing anisotropy of the spin-dephasing at $\alpha = 0$.

We gratefully acknowledge helpful discussions with P. Studerus and A. Fuhrer, and thank R. Leturcq for experimental help. This work was supported by the CTI and the SNF.

-
- [1] G. Dresselhaus, Phys. Rev. **100**, 580 (1955).
 - [2] Y. A. Bychkov and E. I. Rashba, J. Phys. C **17**, 6039 (1984).
 - [3] S. Datta and B. Das, Appl. Phys. Lett. **56**, 665 (1990).
 - [4] J. Schliemann, J. C. Egues, and D. Loss, Phys. Rev. Lett. **90**, 146801 (2003).
 - [5] J. Nitta *et al.*, Phys. Rev. Lett. **78**, 1335 (1997).
 - [6] S. J. Papadakis *et al.*, Science **283**, 2056 (1999).
 - [7] J. B. Miller *et al.*, Phys. Rev. Lett. **90**, 076807 (2003).
 - [8] M. Scheid *et al.*, Phys. Rev. Lett. **101**, 266401 (2008).
 - [9] V. V. Bel'kov *et al.*, Phys. Rev. Lett. **100**, 176806 (2008).
 - [10] S. D. Ganichev *et al.*, Phys. Rev. Lett. **92**, 256601 (2004).
 - [11] M. I. D'yakonov and V. I. Perel', Sov. Phys. Solid State **13**, 3023 (1971).
 - [12] O. Z. Karimov *et al.*, Phys. Rev. Lett. **91**, 246601 (2003).
 - [13] A. V. Larionov and L. E. Golub, Phys. Rev. B **78**, 033302 (2008).
 - [14] L. Meier *et al.*, Nat. Phys. **3**, 650 (2007).
 - [15] G. Salis *et al.*, Phys. Rev. Lett. **79**, 5106 (1997).
 - [16] J. Kainz, U. Rössler, and R. Winkler, Phys. Rev. B **70**, 195322 (2004).
 - [17] G. Salis *et al.*, Nature **414**, 619 (2001).
 - [18] M. Studer *et al.*, Phys. Rev. B **79**, 045302 (2009).
 - [19] R. S. Calsaverini *et al.*, Phys. Rev. B **78**, 155313 (2008).
 - [20] G. Salis *et al.*, Phys. Rev. B **59**, R5304 (1999).
 - [21] S. Döhrmann *et al.*, Phys. Rev. Lett. **93**, 147405 (2004).
 - [22] M. J. Yang *et al.*, Phys. Rev. B **47**, 6807 (1993).
 - [23] R. Winkler, *Spin-Orbit Coupling Effects in Two-Dimensional Electron and Hole Systems* (Springer,

Berlin, 2003).

- [24] J. J. Krich and B. I. Halperin, Phys. Rev. Lett. **98**, 226802 (2007).
- [25] For an overview see in the supplementary material of Ref. 24